Available online at www.sciencedirect.com
ScienceDirect
Earth and Planetary Science Letters 264 (2007) 208 – 225
EPSL
www.elsevier.com/locate/epsl

Low-temperature isotopic fractionation of uranium

Claudine H. Stirling [a,*], Morten B. Andersen [a,1], Emma-Kate Potter [a], Alex N. Halliday [b]

[a] *Institute for Isotope Geology and Mineral Resources, Department of Earth Sciences, ETH, 8092 Zürich, Switzerland*
[b] *Department of Earth Sciences, University of Oxford, Oxford OX1 3PR, UK*

Received 1 December 2006; received in revised form 14 August 2007; accepted 21 September 2007
Available online 29 September 2007
Editor: H. Elderfield

Abstract

Uranium is the heaviest naturally occurring element and isotope fractionation between ^{235}U and ^{238}U is not normally considered significant given the small ~1% difference in mass. It is therefore usual to assume that ^{238}U/^{235}U is constant in the terrestrial environment and equal to 137.88. We have developed experimental protocols for the precise measurement of ^{235}U/^{238}U by multiple-collector ICPMS (MC-ICPMS) and have analyzed a suite of samples formed in a range of low-temperature environments. Using a high-purity ^{233}U–^{236}U double spike to internally monitor the large (percent-level) but essentially constant instrumental mass bias effects that are inherent to plasma source mass spectrometry, we are able to resolve variations in ^{235}U/^{238}U at the 0.4 epsilon level (2σ; 1 epsilon = 1 part in 10,000) on sample sizes comprising 50 ng of uranium. Here we demonstrate sizeable (13 epsilon units) natural variability in ^{235}U/^{238}U, exceeding the analytical reproducibility by more than an order of magnitude. Compositions that are both isotopically heavier and lighter than our terrestrial standard, by 4 and 9 epsilon units respectively, are observed. The largest excursions are found in speleothem samples. Furthermore, ^{235}U/^{238}U appears broadly correlated with ^{234}U/^{238}U in samples showing the most extreme isotopic compositions. The present study investigates the role of abiotic processes in fractionating ^{235}U from ^{238}U. Sequential leaching experiments of U-rich minerals indicate that mineral weathering is a possible mechanism by which ^{235}U can be fractionated from ^{238}U in groundwaters and incorporated into speleothems. The observed variability in ^{235}U/^{238}U indicates that uranium isotopes may offer the potential to monitor new reaction pathways, such as those activated during the redox transition between the U(IV) and U(VI) oxidation states. Experiments involving the redox transition of U(VI) to U(IV) in the presence of zero-valent zinc did not produce a resolvable shift in ^{235}U/^{238}U towards anomalous values, although fractionation need not occur if the reaction is governed by a fast kinetic process. Our observations have a direct impact on the U-series and U–Th–Pb chronometers, when applied to samples formed in low-temperature environments, as these chronometers currently assume an invariant ^{238}U/^{235}U equal to 137.88.

Keywords: uranium isotopes; MC-ICPMS; ^{235}U/^{238}U; fractionation; low-temperature

1. Introduction

Uranium is the heaviest naturally occurring element on Earth and, together with the other actinides, was produced over the lifetime of the galaxy by rapid neutron capture or "*r*-process" stellar nucleosynthesis, then incorporated into

* Corresponding author. Now at: Department of Chemistry, University of Otago, P.O. Box 56, Dunedin, New Zealand. Tel.: +64 3 479 7932; fax: +64 3 479 7906.
E-mail address: cstirling@chemistry.otago.ac.nz (C.H. Stirling).
[1] Now at: Department of Earth Sciences, University of Bristol, Bristol BS8 1RJ, UK.

0012-821X/$ - see front matter © 2007 Elsevier B.V. All rights reserved.
doi:10.1016/j.epsl.2007.09.019

the Earth and planets during the formation of the solar system more than 4.5 billion years ago. Uranium is dominated by three naturally occurring isotopes, ^{238}U, ^{235}U and ^{234}U, and two primary oxidation states with very different solubilities. Under oxidizing conditions in the marine environment, U is typically present in the hexavalent U(VI) form as the large, divalent uranyl ion UO_2^{2+} and highly mobile, forming soluble complexes, primarily with carbonate and phosphate (Ivanovich and Harmon, 1992). In reducing environments, U occurs in the tetravalent U(IV) state, forming relatively insoluble complexes with hydroxides, hydrated fluorides, and phosphates (Ivanovich and Harmon, 1992).

In terms of radioactive properties, ^{238}U ($t_{1/2}$=4.5 billion years) is the parent nuclide of the ^{238}U-decay series, which ultimately decays to stable ^{206}Pb via a series of intermediate nuclides, of which ^{234}U ($t_{1/2}$= 245,000 years) and ^{230}Th ($t_{1/2}$=76,000 years) are the two longest-lived species, while ^{235}U is the parent nuclide of the ^{235}U-decay series, which decays to stable ^{207}Pb with a characteristic half-life of 700 million years via ^{231} Pa ($t_{1/2}$=31,000 years) and a series of shorter lived daughters. The extremely long billion year half-lives characterizing ^{238}U and ^{235}U decay make the ^{238}U–^{206}Pb and ^{235}U–^{207}Pb parent–daughter systems extremely useful for elucidating the earliest history of the solar system (Amelin et al., 2002; Baker et al., 2005), the formation of Earth's atmosphere and hydrosphere (Nutman et al., 1997), and subsequent terrestrial processing via ongoing tectonic, magmatic, metamorphic and glacial events throughout geological time and into the Quaternary (DeCelles et al., 2000). The ten to one hundred thousand year half-lives characterizing ^{238}U–^{234}U–^{230}Th (or U-series) and ^{235}U–^{231}Pa decay have been widely utilized as chronometers and tracers in the environmental, archaeological, and geochemical sciences, most notably with respect to paleoclimate and magmatic time-scale research spanning the last half million years of the late Quaternary (Edwards et al., 1987; Esat et al., 1999; Stirling et al., 2001; Gallup et al., 2002; Lundstrom, 2003; Turner et al., 2003; Robinson et al., 2004b). Moreover, ^{247}Cm ($t_{1/2}$=15.6 million years), the short-lived and presently extinct precursor nuclide of the ^{235}U decay series, has been used in cosmochemistry to constrain the evolution of the early solar system (Chen and Wasserburg, 1980, 1981; Stirling et al., 2005; Stirling et al., 2006).

Permil- to percent-level variations in ^{234}U/^{238}U have been widely documented in low-temperature terrestrial environments reflecting disequilibrium in the decay series. For example, seawater contains a 15% excess of ^{234}U with respect to the abundances expected at radioactive equilibrium (Chen et al., 1986), and more extreme ^{234}U excesses can be found in rivers and groundwaters (Andersson et al., 1998; Reynolds et al., 2003). Such large effects arise because the radioactive decay of ^{238}U to ^{234}U (via ^{234}Th and ^{234}Pa) through the emission of one α-particle and two β-particles results in extensive damage to the crystal lattice; the ^{234}U daughter is often ejected from its original location by α-recoil rendering it more susceptible to oxidation and selective leaching than its lattice-bound ^{238}U parent (Kigoshi, 1971), and may even be directly released into the surrounding medium provided the mineral grain size is sufficiently small (DePaolo et al., 2006).

In contrast, significant permil-level mass-dependent thermodynamic isotopic fractionations, resulting from small differences in the zero-point vibrational frequencies between isotopically light and heavy substances (Bigeleisen and Mayer, 1947; Urey, 1947; Richet et al., 1977), as has been observed in recent years in the heavy stable isotope systems of, for example, iron (Anbar, 2004), zinc (Marechal and Albarede, 2002) and copper (Marechal and Albarede, 2002), are not expected to be detectable in U due to its heavy mass. As opposed to loosely bound ^{234}U, both ^{235}U and ^{238}U are strongly bound to the crystal lattice. The small ~1% difference between the masses of these nuclides and the concomitant scaling of the vibrational fractionation shift with $\delta M/M^2$ (Bigeleisen and Mayer, 1947) limits mass-dependent fractionation effects in uranium per a.m.u. to only one twentieth of those found in iron. It is therefore usual to link the ^{238}U and ^{235}U decay chains through the inherent assumption that the isotopic ratio between the ^{238}U and ^{235}U parent nuclides is invariant throughout the Earth, and moreover, across the entire solar system, being equal everywhere to 137.88 at the present day (Cowan and Adler, 1976; Steiger and Jaeger, 1977). A rare exception to this has been documented at the site of the Oklo fossil nuclear reactors in West Africa (Proceedings of an International Symposium on the Oklo Phenomenon, 1975). Cowan and Adler (1976) proposed a natural variability of 0.03% in ^{235}U/^{238}U for a range of uranium ores.

In recent years, thallium, a heavy element with stable isotopes at masses 203 and 205, has been shown to display large, permil-level ^{205}Tl/^{203}Tl variability (Rehkämper et al., 2002; Rehkämper and Nielsen, 2004; Nielsen et al., 2005; Nielsen et al., 2006), despite the small mass difference between ^{205}Tl and ^{203}Tl. Similarly large isotopic fractionations have been observed for mercury with respect to the ^{202}Hg/^{198}Hg ratio (Smith et al., 2005; Xie et al., 2005). Thallium and

mercury isotopic fractionations have recently been investigated in the context of mass-independent isotopic fractionation associated with the nuclear field shift effect. This arises because of varying nuclear volumes and electron density distributions between different isotopes of the same element (Schauble, 2007), which change as a function of oxidation state. In contrast to the above-mentioned vibrational effects, the nuclear field shift effect does not scale with $\delta M/M^2$. Moreover, it is predicted to have a particularly strong effect on the heavy masses. Therefore, it is not unreasonable to propose that $^{235}U/^{238}U$ may show similar variability to $^{205}Tl/^{203}Tl$ and $^{202}Hg/^{198}Hg$ in certain terrestrial environments. For example, in the U(IV)–U(VI) exchange reaction, the nuclear field effect is predicted to be three times as large and of opposite sign to the vibrational energy term (Bigeleisen, 1996), offering the potential to detect variations in $^{235}U/^{238}U$ in natural environments.

We have developed experimental protocols for the precise measurement of $^{235}U/^{238}U$ by multiple-collector magnetic sector ICPMS (MC-ICPMS). Using a Nu Instruments Nu Plasma MC-ICPMS, we are able to resolve variations in $^{235}U/^{238}U$ at the 0.4 epsilon level ($2\sigma_M$; 1 epsilon = 1 part in 10^4) on sample sizes comprising 50 ng of uranium. High quality U measurements are possible because we have used a high-purity

Table 1
Uranium isotopic data for natural samples formed in "low-temperature" terrestrial environments

Sample type [a]	Sample name [b]	Aliquot [c]	$\varepsilon^{235}U$ [d]	$\delta^{234}U_{meas}$ [e]
Seawater	Makarov Basin	(1)	4.4 ± 0.7	147
		(2)	4.5 ± 1.5	147
	H-6 North Sea	(1)	5.7 ± 0.9	147
		(2)	5.0 ± 0.7	147
	Oeno Pacific		4.1 ± 0.4	147.5 ± 0.9
	Henderson Pacific		5.0 ± 0.7	147.1 ± 0.3
Modern coral	Oeno Pacific		5.0 ± 1.2	146.8 ± 0.3
Fossil coral	AC4-7		4.6 ± 0.9	103.9 ± 0.9
	U6-11.1	(1)	3.7 ± 0.6	119.3 ± 0.7
		(2)	4.0 ± 0.7	119.3 ± 0.7
	U6-11.3	(1)	3.8 ± 0.5	99.4 ± 0.5
		(2)	4.2 ± 0.7	99.4 ± 0.5
	NB-D-4		5.1 ± 0.9	63.7 ± 0.3
	NB-D-7		6.4 ± 1.3	64.0 ± 0.3
	NEB-1C		3.9 ± 1.0	72.6 ± 0.3
Fe–Mn deposit	JMN-1	(1)	6.8 ± 0.7	–
		(2)	5.7 ± 0.9	–
Chimney	ETH	(1)	8.2 ± 0.7	239.4 ± 0.8
		(2)	8.4 ± 0.7	239.4 ± 0.8
Speleothem	KOZ (A)	(1)	−4.4 ± 0.9	−464.5 ± 0.5
		(2)	−3.8 ± 0.8	−464.5 ± 0.5
	KOZ (B)		−2.9 ± 0.9	−464.5 ± 0.5
	SPA-43	(1)	6.3 ± 0.8	15.0 ± 0.5
		(2)	6.5 ± 0.9	15.0 ± 0.5
			7.0 ± 1.1	15.0 ± 0.5
			5.9 ± 2.8	15.0 ± 0.5
	Argentarola	(1)	4.2 ± 0.7	467.5 ± 0.8
		(2)	5.2 ± 0.7	467.5 ± 0.8
		(3)	4.9 ± 0.7	467.5 ± 0.8
	FAB-LIG	(1)	2.5 ± 0.8	83.3 ± 1.2
		(2)	2.0 ± 0.9	83.3 ± 1.2
River	Danube	(1)	2.3 ± 0.6	–
		(2)	2.0 ± 0.5	–
		(3)	2.4 ± 0.5	–
Shale	Sco	(1)	2.6 ± 0.6	–
		(2)	2.9 ± 0.7	–
Uraninite	HU-1		5.6 ± 0.9	0.0 ± 0.3
	CU-1		2.0 ± 0.7	0.1 ± 0.3
	CZ-1		1.0 ± 0.7	1.4 ± 0.3

^{236}U–^{233}U double spike to internally monitor the large (percent-level) but essentially constant instrumental mass bias effects that are inherent to plasma source mass spectrometry.

In the present study, we present new observations for a suite of "low-temperature" samples, in order to investigate potential $^{235}U/^{238}U$ fractionations in near-surface terrestrial environments. These new data supplement observations acquired previously for terrestrial and meteoritic samples formed in high-temperature environments (Stirling et al., 2005; Stirling et al., 2006). Sizeable, epsilon-level $^{235}U/^{238}U$ fractionations are observed, exceeding the analytical reproducibility by more than an order of magnitude.

Uranium isotopic fractionation in $^{235}U/^{238}U$ may thus offer the potential to monitor new reaction pathways, such as those activated during biological cycling and redox processing occurring, for example, during mineralization, weathering, and the transition between the U(IV) and U (VI) oxidation states, offering new insight into the processes at work. Natural variability in $^{235}U/^{238}U$ will also have a direct impact on the accuracy of the U-series and ^{235}U–^{231}Pa short-lived Quaternary chronometers, the U–Th–Pb chronometers, and the Cm–U "*r*-process" cosmochronometer, which currently assume that $^{235}U/^{238}U$ is invariant in all terrestrial and extraterrestrial environments. For example, models of solar system formation formulated on the basis of the ^{207}Pb–^{206}Pb and ^{247}Cm–^{235}U chronometers are often based on relative age differences of only a few million years (Amelin et al., 2002; Amelin, 2005; Baker et al., 2005), and may need to be reconsidered if $^{235}U/^{238}U$ fractionation is found. Similarly, the chronologies of Quaternary paleoclimate records (Winograd et al., 1992; Esat et al., 1999; Stirling et al., 2001; Gallup et al., 2002; Robinson et al., 2002) need only to be shifted by ~1000 years towards incorrect values to drastically alter our understanding of the dynamics and mechanisms driving Quaternary climate change.

In the present study, viable mechanisms to account for the natural $^{235}U/^{238}U$ variability shown by the analyzed samples are investigated in the context of abiotic processes. Potential isotopic fractionation of $^{235}U/^{238}U$ linked to biological processing is explored in a separate study.

Notes to Table 1

[a] For the ferromanganese deposits, approximately 50–120 mg of sample power was leached for ~15 min on a warm hotplate with 6 N HCl to dissolve the manganese oxide, which was then separated from any undissolved detrital material by centrifugation. The coral, speleothem and chimney samples were prepared as small chips, and surface contaminants, if any, were removed by ultrasonic agitation with distilled ethanol. These samples were covered with H_2O, dissolved by the stepwise addition of concentrated HNO_3, and if necessary, centrifuged to remove any undissolved detrital material. The river and seawater samples were acidified to a pH of 2 and filtered through a 0.45 mm Millipore filter directly after collection, then 100–250 ml aliquots were extracted and co-precipitated with iron by the stepwise addition of ammonia. The resulting Fe-flocculate was dissolved in concentrated HNO_3, following centrifugation and removal of the supernate. All uraninites and U standards were received as solutions and require no further pre-treatment. Makarov Basin seawater was collected during the AO-01 expedition. The North Sea seawater sample is characterized in Andersson et al. (1992, 1995). The Danube River sample is described in Nielsen et al. (2005). The SPA 43 speleothem was sampled from Spannagel Cave, Austria (Spoetl et al., 2002).

[b] (A) and (B) refer to replicate analyses on independently processed pieces of the same sample.

[c] Repeat analyses on the same solution aliquot are indicated by (1) through (9).

[d]

$$\varepsilon^{235}U = \left(\left[\frac{\left(^{235}U/^{238}U\right)_{sample}}{\left(^{235}U/^{238}U\right)_{standard}}\right] - 1\right) \times 10^4$$

where $(^{235}U/^{238}U)_{standard}$ denotes the mean value determined for CRM 145 U during the analysis session. Note that our previously published $\varepsilon^{235}U$ measurements are based on normalization to the chondritic average of $4.6 \pm 0.4\varepsilon$ (Stirling et al., 2005; Stirling et al., 2006). All $\varepsilon^{235}U$ measurements were corrected for both the contributions of ^{235}U and ^{238}U present in the ^{236}U–^{233}U double spike and for instrumental mass fractionation, using the measured $^{236}U/^{233}U$ normalized to the true value. Uncertainties are $2\sigma_M$ and include the contribution from the daily mean of the standard.

[e]

$$\delta^{234}U = \left(\left[\frac{\left(^{234}U/^{238}U\right)_{sample}}{\left(^{234}U/^{238}U\right)_{equilibrium}}\right] - 1\right) \times 10^3$$

where λ_{234} and λ_{238} denote the decay constants for ^{234}U and ^{238}U, respectively. The $\lambda_{238}/\lambda_{234}$ ratio of the decay constants represents the $^{234}U/^{238}U$ atomic ratio at radioactive secular equilibrium, determined as 5.4891×10^{-5} (Cheng et al., 2000). Unless measured, the nominal marine $\delta^{234}U$ of 147‰ (Chen et al., 1986; Delanghe et al., 2002; Robinson et al., 2004a; Andersen et al., 2007) is adopted for the seawater samples. Uncertainties are $2\sigma_M$.

2. Experimental protocols

2.1. Chemical preparation

A double-spiking procedure, using a mixed ^{236}U–^{233}U spike, is employed to allow instrumental mass fractionation to be reliably corrected internally and at high precision (Stirling et al., 2005; Stirling et al., 2006). For powdered or fragmented samples, the ^{236}U–^{233}U tracer is added prior to acid digestion, and for acid-leached samples, the tracer is added to the leachate immediately following separation from the precipitate by

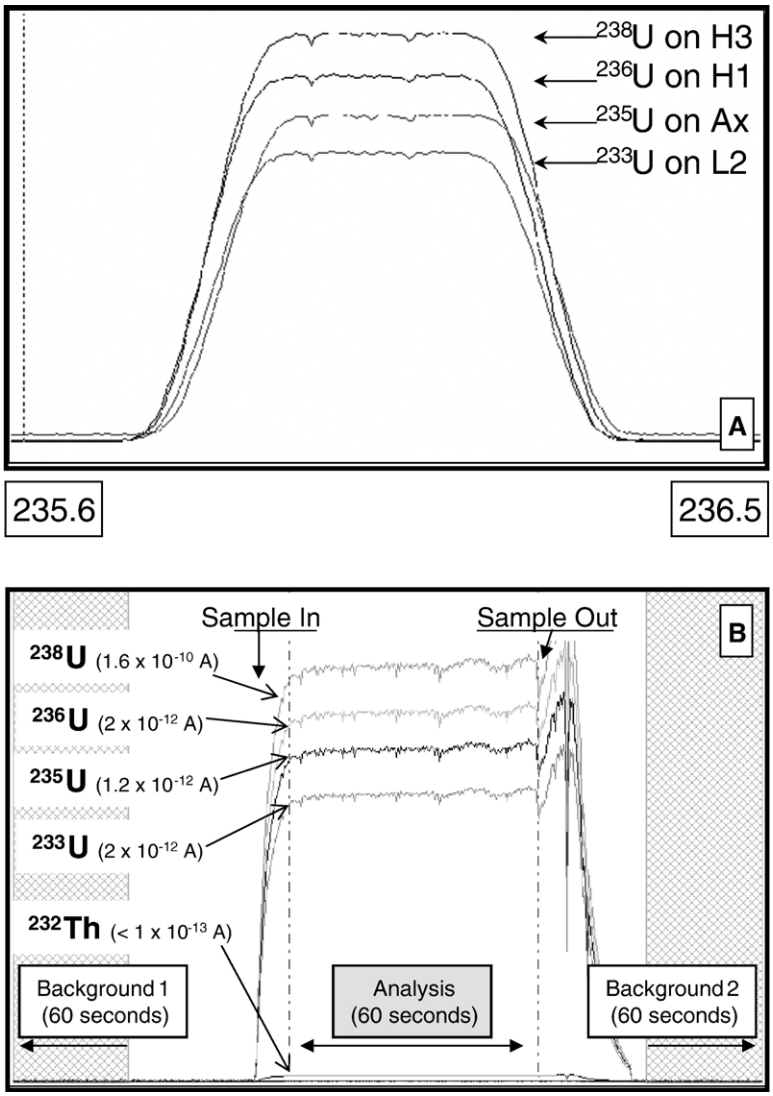

Fig. 1. (A) Uranium peak shapes and collector alignment (achieved using zoom optics) for $^{235}U/^{238}U$ measurement using a double spike derived of high-purity ^{233}U–^{236}U to monitor instrumental mass fractionation. Mass resolution $\Delta M/M$ is 400. Short-term oscillations in ion beam intensity inherent to ICPMS, referred to as "plasma flicker" can be seen. The peaks represent 8 integrated scans over a mass range of 0.9 a.m.u. ^{235}U is monitored in the central axial Faraday collector, while ^{238}U, ^{236}U, ^{233}U and ^{232}Th are monitored simultaneously on H3, H1, L2 and L3, respectively. (B) Multiple-Faraday $^{235}U/^{238}U$ measurement of a meteorite sample, conducted using the "time-resolved" software supplied with the Nu Plasma MC-ICPMS. Initially, the electronic noise of the Faraday collectors is monitored as a 60-second zero measurement (Background 1), while the ion beams are deflected off-axis. Thereafter, the sample or standard solution is introduced and the ion beams "grow in" and stabilize. Data are then acquired over a ~1 min period as a series of 0.2 s integrations giving ~300 ratios. The sample is then removed and a second zero is measured for 60 s (Background 2). The on-peak data are corrected for the electronic background by linear interpolation of the two zero measurements. The measured isotope ratios are then calculated off-line and corrected for both the contributions of natural U isotopes present in the ^{233}U–^{236}U spike and instrumental mass fractionation (by normalization against $^{236}U/^{233}U$) using a 2σ rejection criteria. In this example, measurement intensities are 1.6×10^{-10} A for ^{238}U, 2×10^{-12} A for ^{236}U and ^{233}U, 1.2×10^{-12} A for ^{235}U and $<1\times10^{-13}$ A for ^{232}Th.

centrifugation. Dissolution protocols are described in the notes to Table 1. Following spiking, all samples are treated with highly oxidizing aqua regia, H_2O_2–HNO3 or $HClO_4$, or a combination of the above, and refluxed, in order to remove organic material and promote sample-spike equilibration. After the final cycle of evaporation to dryness, the samples are re-dissolved in 1.5 N HNO_3 in preparation for ion-exchange chemical separation procedures. Uranium is chemically extracted from the sample matrix using TRU.Spec ion-exchange resin (Eichrom) and separation protocols modified from Luo et al. (1997). The uranium fraction is further purified using UTEVA ion-exchange resin (Eichrom), following protocols reported in Potter et al. (2005b). This provides an effective separation of U from Th which is required to minimize interferences on ^{233}U caused by hydrides of ^{232}Th (^{232}ThH$^+$). Following evaporation to dryness, the U fraction is re-dissolved in 0.25 N HCl + 0.05 N HF in preparation for mass spectrometric analysis. The total U chemistry blank is at the fg–pg level and thus has a negligible effect on the measured U isotopic composition.

2.2. Measurement protocols

Uranium ^{235}U/^{238}U and ^{234}U/^{238}U isotopic measurements were performed on a Nu Instruments Nu Plasma MC-ICPMS (Belshaw et al., 1998; Rehkämper et al., 2001; Goldstein and Stirling, 2003; Halliday et al., in press) coupled to an Aridus or MCN 6000 desolvating nebulizer (CETAC Technologies) using protocols reported in (Stirling et al., 2005; Stirling et al., 2006) and (Andersen et al., 2004; Andersen et al., 2007), respectively.

Uranium ^{235}U/^{238}U isotopic data were collected as a single static measurement by simultaneously monitoring ^{233}U ($1.5–2.0\times10^{-12}$ A), ^{235}U ($0.8–1.1\times10^{-12}$ A), ^{236}U ($1.5–2.0\times10^{-12}$ A) and ^{238}U ($1.2–1.6\times10^{-10}$ A) on an array of Faraday collectors operating with 10^{11} Ω resistors (Fig. 1B). ^{232}Th was also measured to monitor ^{232}ThH$^+$ production, which interferes on ^{233}U (^{232}Th H$^+$/^{232}Th ~ 15 ppm). In practice, UTEVA chemistry achieves a very clean separation of U from Th (U/Th > 1000) so that Th hydride interferences, as well as other potential interferences, such as platinum argides and mercury chlorides on ^{235}U, were negligible. Abundance sensitivity

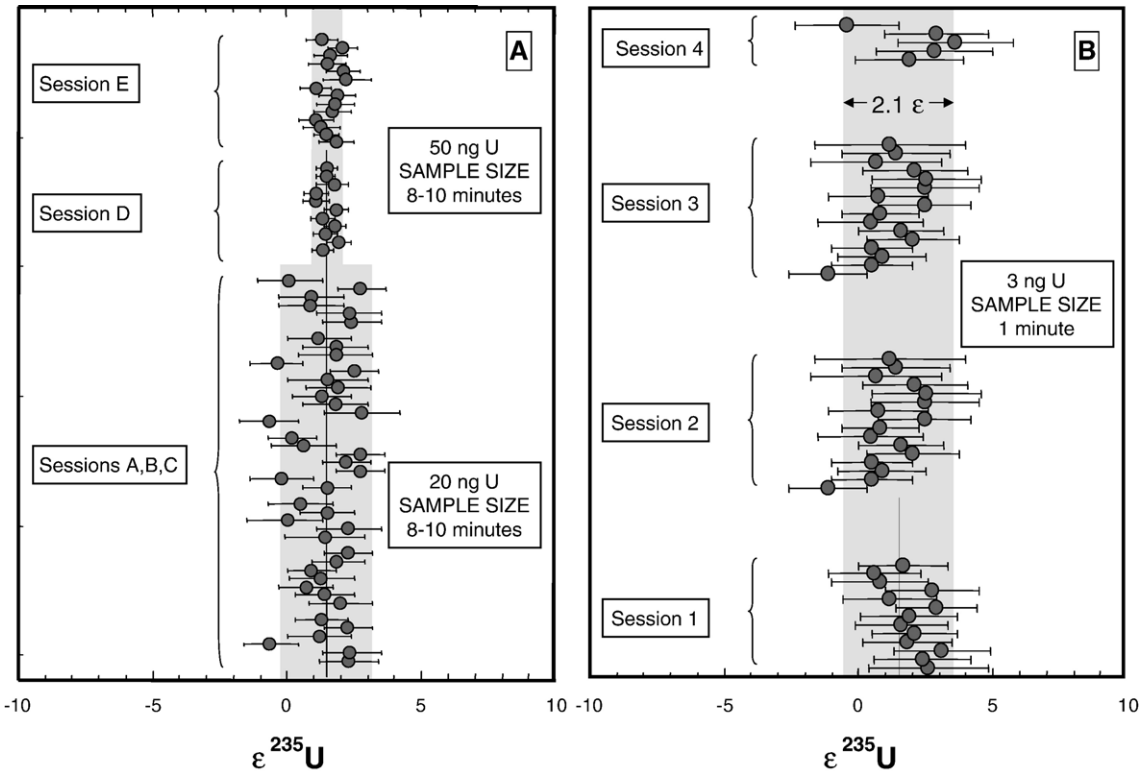

Fig. 2. Repeat ε^{235}U measurements for U standard material. Within-run analytical precision is typically (A) ±0.4ε for 50 ng U load sizes and ±1–2ε for 20 ng U sample loads analyzed for 8–10 min and, and (B) ±2ε for load sizes corresponding to 3 ng of total U analyzed for 1 min. Repeat analyses acquired over a protracted period spanning multiple measurement sessions are shown. The long-term external reproducibility, represented by the shaded band, is typically comparable to the 2σ internal precision on individual measurements but can be marginally larger due to the limited $<1.2\times10^{-12}$ A intensity of the ^{235}U ion beam and its dependence on the daily stability of the MC-ICPMS instrument.

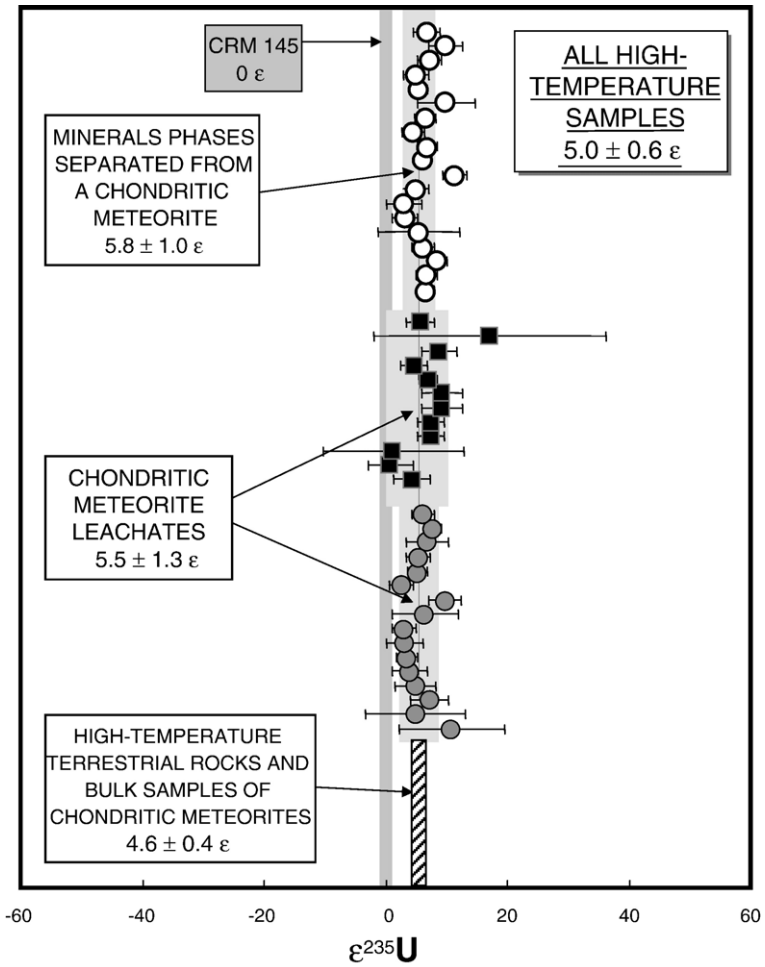

Fig. 3. ε^{235}U for separated mineral phases (open circles) and acid-etched leachates (closed circles and squares) extracted from a suite of chondritic meteorites, as well as bulk samples of high-temperature terrestrial rocks and chondritic meteorites (represented by the hatched band), reported in (Stirling et al., 2005; Stirling et al., 2006). The 2σ external reproducibility of the CRM 145 U standard for a comparable U load size (represented by the shaded band) is shown for reference. Note the extended 120ε range represented by the *x*-axis compared with the 10–20ε range displayed in most other figures. Note that the ε^{235}U results for meteorites reported in Stirling et al. (2005, 2006) were normalized instead to the bulk chondritic value, which is offset by +4.6±0.4ε (2σ_M) with respect to the ε^{235}U determined form CRM 145.

(defined as the contribution at mass 237 from the large ^{238}U ion beam) is <2 ppm and the contribution to each of the minor ^{233}U, ^{235}U and ^{236}U isotopes from ^{238}U peak tailing was negligible. Fig. 1A shows typical peak shapes and collector alignment (achieved using zoom optics) for our measurement routines. On-peak analyses were conducted over a 1 min (Fig. 1B) to 10 min acquisition period, using analysis protocols described in Stirling et al. (2005, 2006), the duration of the measurement depending on sample size availability. At the end of each cycle, all ^{235}U/^{238}U ratios were corrected for both the contributions of ^{235}U and ^{238}U present in the ^{236}U–^{233}U mixed spike and for instrumental mass fractionation, using the measured ^{236}U/^{233}U normalized to the true value and the exponential mass fractionation law (Hart and Zindler, 1989; Habfast, 1998). Details of the ^{236}U/^{233}U calibration of the mixed spike have been discussed previously (Stirling et al., 2005). Washout between sample/standard measurements was achieved using sequential solutions of 0.3 N HCl+0.1 N HF and 0.25 N HCl+0.05 N HF. To maintain consistency with previously published ^{235}U/^{238}U data (Chen and Wasserburg, 1980; Stirling et al., 2005), all ^{235}U/^{238}U measurements have been reformulated into ε-notation, with respect to the isotopic composition of the CRM 145 uranium metal standard (Stirling et al., 2005), as defined in Eq. (1) below. Using this nomenclature, isotopically "heavy" samples are characterized by more negative ε^{235}U values and

conversely, isotopically "light" samples display more positive ε^{235}U values. It is important to note that our previously published meteoritic data (Stirling et al., 2005; Stirling et al., 2006) were normalized instead to the value determined for bulk chondritic meteorites, which is offset by $+4.6\pm0.4\varepsilon$ ($2\sigma_M$) with respect to the ε^{235}U determined for CRM 145. This offset should be kept in mind when directly comparing the data presented here with that reported previously. Similarly, all reported ^{234}U/^{238}U measurements have been reformulated into δ-notation, with respect to the ^{234}U/^{238}U value at isotopic secular equilibrium, as defined in Eq. (2) below. All reported uncertainties are quoted as $2\sigma_M$.

Table 2
Experimental uranium isotopic data

Sample [a]	Fraction [b]	Aliquot [c]	ε^{235}U [d]
Sequential acid leaching			
Uraninite CZ	0.1 N HNO_3	(1)	1.2±0.6
		(2)	1.5±0.7
	0.7 N HNO_3	(1)	0.3±0.6
		(2)	1.3±0.6
	1.4 N HNO_3	(1)	1.6±0.5
		(2)	0.3±0.5
	Bulk (A)	(1)	0.6±0.4
		(2)	0.8±0.5
		(3)	1.2±0.6
		(4)	1.2±0.6
	Bulk (B)	(1)	1.7±0.9
		(2)	0.6±0.9
		(3)	0.7±0.9
Euxenite	0.1 N HNO_3	(1)	7.1±0.7
		(2)	8.1±0.6
		(3)	6.7±0.8
		(4)	6.3±0.8
	0.7 N HNO_3	(1)	6.8±0.8
		(2)	7.2±0.8
		(3)	6.7±0.5
	1.4 N HNO_3	(1)	6.8±0.7
		(2)	6.3±0.8
		(3)	6.7±0.7
		(4)	8.1±0.7
	9 N HCl-A	(1)	7.8±0.8
		(2)	8.9±0.8
	9 N HCl-B	(1)	12.3±0.7
		(2)	10.8±0.7
	HNO_3–HCl–HF (incomplete)	(1)	11.0±0.7
		(2)	10.4±0.7
Zircon	0.1 N HNO_3		4.5±0.7
	0.7 N HNO_3	(1)	6.3±0.7
		(2)	5.4±0.7
	1.4 N HNO_3	(1)	5.1±0.7
		(2)	5.0±0.6
Oxidation–reduction			
CRM 145 (O)	80 ppb U(VI)	(1)	0.3±0.6
		(2)	0.0±0.4
		(3)	−0.2±0.6
		(4)	−0.4±0.6
		(5)	0.3±0.6
		(6)	−0.4±0.5
		(7)	0.5±0.6
		(8)	0.0±0.6
		(9)	−0.2±0.5
CRM 145 (A)	32 ppb U(VI)	(1)	0.1±0.6
		(2)	0.5±0.5
CRM 145 (B)	32 ppb U(VI)		0.7±0.8
CRM 145 (C)	32 ppb U(VI)	(1)	0.2±0.6
		(2)	0.3±0.6

Notes to Table 2 (see notes to Table 1)

[a] For the oxidation–reduction experiments, CRM 145 (O) denotes the initial 80 ppb starting solution of CRM 145, adjusted with MQ H_2O to a pH of 5.5, and contains oxidized U(VI) at a concentration of 80 ppb. Zero-valent zinc was added to three independent aliquots of CRM 145(O) to reduce U(VI) to U(IV). After 3 h, the residual solutions, referred to as CRM 145 (A), (B) and (C), were removed. In each, the concentration of U(VI) was found to be ~32 ppb, implying a 60% reduction of U(VI) to U(IV).

[b] For the sequential leaching experiments, reagents of progressing strength were used in an attempt to preferentially dissolve isotopically light ^{235}U from the mineral surface with respect to ^{238}U, or to sequentially dissolve different mineral zones with potentially varying ε^{235}U. The following sequential dissolution procedure was employed for the euxenite: (1) 0.1 N HNO_3; (2) 0.7 N HNO_3; (3) 1.4 N HNO_3; (4) 9 N HCl-1; (5) 9 N HCl-2; and (6) HNO_3–HCl–HF. The final HNO_3–HCl–HF acid digestion step did not result in complete dissolution of the euxenite, as a residue remained. The uraninite and zircon were subjected to the first three nitric acid leach steps only. The uraninite underwent total dissolution with HNO_3-trace HF.

$$\varepsilon^{235}\mathrm{U} = \left(\left[\frac{\left(^{235}\mathrm{U}/^{238}\mathrm{U}\right)_{\mathrm{sample}}}{\left(^{235}\mathrm{U}/^{238}\mathrm{U}\right)_{\mathrm{standard}}}\right] - 1\right) \times 10^4 \qquad (1)$$

$$\delta^{234}\mathrm{U} = \left(\left[\frac{\left(^{234}\mathrm{U}/^{238}\mathrm{U}\right)_{\mathrm{sample}}}{\left(^{234}\mathrm{U}/^{238}\mathrm{U}\right)_{\mathrm{equilibrium}}}\right] - 1\right) \times 10^3 \qquad (2)$$

3. Standard and reference measurements

An in-house uranium standard, double spiked and chemically processed in the same way as the samples, was used to assess the performance of our analytical protocols for ^{235}U/^{238}U measurement. The results for repeat measurements of ε^{235}U, acquired over several independent measurement sessions, are shown in Fig. 2. Fig. 2A shows that variations in ^{235}U/^{238}U can be resolved at the 0.4ε (or 40 ppm; 2σ) level using sample sizes equivalent to ~50 ng of uranium and analysis

times of ~10 min. Fig. 2B demonstrates that highly reproducible data can also be acquired by analyzing a concentrated solution for a short duration interval of only 1 min when sample size is limited, routinely achieving 2σ analytical uncertainties of ± 1–2ε for ^{238}U load sizes corresponding to <3 ng (Stirling et al., 2006).

With the exception of only one or two outlying data points, uranium isotopic data for a range of terrestrial and meteoritic samples formed in high-temperature environments (Fig. 3), normalized to CRM 145, show no resolvable excursions away from the mean value of $+4.6\pm0.4\varepsilon$ ($2\sigma_M$) determined for chondritic meteorites (Stirling et al., 2005; Stirling et al., 2006), but are systematically offset from the ε^{235}U value determined for CRM 145 by $+5.0\pm0.6\varepsilon$ ($2\sigma_M$). For this dataset, derived predominantly from measurements for meteorite samples with extremely low (ppt-ppb) level U concentrations, our ability to resolve distinct ^{235}U/^{238}U compositions is limited to the $>2\varepsilon$ level when individual data points are considered. Importantly, when the analyzed meteorites are grouped by sample type, in order to instead compare the higher precision mean values associated with each group, the ε^{235}U determinations remain indistinguishable, giving rise to ε^{235}U values of 4.6 ± 0.4, 5.5 ± 1.3, and $5.8\pm1.0\varepsilon$ ($2\sigma_M$) for bulk chondritic meteorites and high-temperature terrestrial materials, chondritic meteorite leachates, and individual mineral phases separated from a chondritic meteorite, respectively. The implication is that no fractionation of ^{235}U from ^{238}U has been resolved in any of the analyzed samples, even at the 1ε level. Our previous high-temperature observations for bulk chondritic meteorites and terrestrial samples, centred about $+4.6\varepsilon$, thus provide a suitable benchmark against which the low-temperature sample suite can be referenced to.

4. Measurements of samples formed in low-temperature environments

Our initial low-temperature sample suite comprises aliquots of seawater and river water, corals, manganese nodule and chimney deposits, anoxic sediment, speleothems and uraninites. Uranium ^{235}U/^{238}U isotopic data for these samples are displayed in Fig. 4 and Table 2.

Four samples of surface seawater, collected from disparate ocean basins in the Arctic region (Makarov Basin and the North Sea) and the Pacific region, display no variability in ε^{235}U at the 1ε-level and yield a mean value of $+4.8\pm0.5\varepsilon$ ($2\sigma_M$). This is identical, within error, to the mean chondritic value of $+4.6\pm0.4\varepsilon$ ($2\sigma_M$) determined for the high-temperature dataset displayed in Fig. 3. Uranium ^{235}U/^{238}U isotopic data for corals, a dolomite chimney sample, and the Fe–Mn nodule, all of which form by co-precipitation processes in the marine environment, are discussed in turn below.

Corals forming in the marine environment have the potential to preserve U isotopic fractionation effects with respect to the above-mentioned seawater value that are associated with (1) the biologically-mediated co-precipitation of U with other trace metals in the water column as they build their Ca-aragonite skeletons, (2) secular variations in the marine ^{235}U/^{238}U, and (3) the post-depositional diagenetic alteration of the coral skeleton, often accompanied by the open-system exchange of U and Th. The latter point is important in the context of the recent debate concerning the mechanisms controlling carbonate diagenesis. Only minor diagenetic alteration results in extreme shifts in the ^{234}U/^{238}U (and ^{230}Th/^{238}U) composition, most likely through ^{234}U (and ^{230}Th) addition, shifting the U-series age determinations to very anomalous values (Bard et al., 1991; Gallup et al., 1994; Stirling et al., 1995; Stirling et al., 1998). Recently, open-system models have been devised (Thompson et al., 2003; Villemant and Feuillet, 2003) to "remove" these diagenetic effects from published U-series observations, in order to re-evaluate the Quaternary sea-level curve for the last two glacial–interglacial cycles (Thompson and Goldstein, 2005, 2006), however, the reliability of such open-system model ages remains uncertain. In the present study, a modern coral, as well as fossil corals formed 125,000 and 330,000 years ago, were analyzed for ε^{235}U. In addition, pristine and altered portions of a ~100,000 year-old fossil coral were analyzed, for the purpose of testing if the extreme isotopic fractionation of ^{234}U/^{238}U could be accompanied by additional fractionation of ^{235}U/^{238}U, the latter of which is presently not accounted for by the open-system models. All samples yielded identical ε^{235}U, within their quoted 2σ error limits, and a mean value of $+4.5\pm0.6\varepsilon$ ($2\sigma_M$) that is indistinguishable from the mean value determined for open ocean seawater. Therefore, these results demonstrate that no ^{235}U/^{238}U fractionation occurs during the formation of Ca-aragonite during coral-building. They also imply that ^{235}U/^{238}U has remained constant in the oceans during the last 330,000 years of the Quaternary, and furthermore, that no fractionation or addition of ^{235}U/^{238}U occurs during diagenetic alteration. Thus, variability in ^{235}U/^{238}U need not be considered further as a diagenetic parameter in open-system U-series age modelling.

The Ca-dolomite chimney, which formed in a hypersaline lagoon in Brazil, has an ε^{235}U of $+8.3\pm0.2\varepsilon$ ($2\sigma_M$), significantly higher than the values obtained for both seawater and the other marine deposits. This may

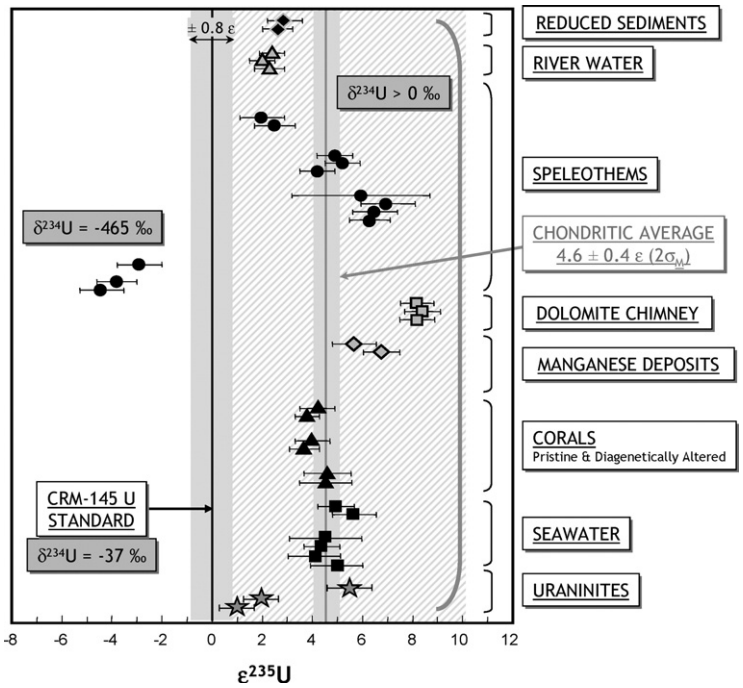

Fig. 4. ε^{235}U for a suite of samples formed in a range of low-temperature terrestrial environments. Results for uraninites (grey stars), modern seawater (black squares), pristine and diagenetically altered fossil corals (black diamonds), manganese nodule (grey circles and grey diamonds) and dolomite chimney deposits (grey squares), speleothems (black circles), river water (grey triangles) and shale, a proxy for anoxic sediment (black diamonds) are shown. The 2σ external reproducibility of the CRM 145 U standard for a comparable U load size (represented by the shaded band) and the mean ε^{235}U value of $+4.6\pm0.4$ ($2\sigma_M$) determined for high-temperature bulk chondritic meteorites and terrestrial samples are shown for reference. Samples with δ^{234}U>0 plot in the hatched region. Note that previously published meteoritic data are reported with respect to the mean chondritic value as opposed to CRM 145 (see the caption to Fig. 3).

reflect ^{235}U/^{238}U offsets experienced during either Ca-dolomite formation, or alternatively during the biologically-mediated reduction of U(VI) to U(IV) induced by sulphate-reducing bacteria, whereby isotopically light ^{235}U is preferentially incorporated into the crystal lattice over heavy ^{238}U.

An older marine sample of Fe–Mn nodule was also analyzed for ^{235}U/^{238}U, motivated by the large, permil-level isotopic fractionations that have been found in thallium between seawater and Fe–Mn deposits, which have ε^{205}Tl values of averaging about -6ε and $+13\varepsilon$, respectively (Rehkämper et al., 2002). These compositional differences have been ascribed to the adsorption of thallium onto the surfaces of Fe–Mn particles during formation (Rehkämper et al., 2002). The manganese nodule analyzed in the present study displays an ε^{205}Tl value of $+6.2\varepsilon$, and an ε^{235}U value of $+6.3\pm1.1\varepsilon$ ($2\sigma_M$), which is marginally shifted by ~1–2ε towards more positive values with respect to the seawater value.

River waters also display wide-ranging Tl isotopic compositions. Thus in the present study, the Danube River sample, which displays an anomalously negative thallium isotopic composition ε^{205}Tl of -6.6ε (Nielsen et al., 2005) (compared with the average riverine composition of ε^{205}Tl$=-2.5\varepsilon$) was analyzed for uranium, yielding an ε^{235}U of $+2.2\pm0.2\varepsilon$ ($2\sigma_M$), marginally shifted by $\sim2\varepsilon$ towards more negative values with respect to seawater, in agreement also with measurements for the analyzed shale, a proxy for anoxic sediment (ε^{235}U$=+2.7\pm0.3\varepsilon$; $2\sigma_M$). Although not definitively resolved from the average terrestrial ε^{235}U composition defined by the high-temperature dataset, the apparent positive correlation between ε^{235}U and ε^{205}Tl in both the marine and riverine samples tentatively suggests a coupled isotopic fractionation between thallium and uranium, perhaps linked by a commonality in the redox chemistries of these two elements. Importantly, the isotopic shift in uranium appears to be in the opposite direction to that shown by thallium, as the preferential uptake of the heavy ^{205}Tl isotope is accompanied by the preferential uptake of the light ^{235}U isotope, and vice versa.

The analyzed uraninite samples show considerable variability in their ε^{235}U compositions, displaying values ranging from $+1.0$ to $+5.6\varepsilon$ with respect to CRM 145. In particular, eight measurements of the widely utilized U-

series standard HU-1 yield an ε^{235}U value of +5.6±0.7ε (2σ_M) with respect to CRM 145, which is identical within error to the average terrestrial value of 5.0±0.6ε (2σ_M). However, the greatest variability in ^{235}U/^{238}U is found in Quaternary-aged speleothems precipitated from groundwater (Fig. 4). Five independent samples of speleothems display an ε^{235}U variability of ~13ε, which exceeds the analytical reproducibility by up to a factor of ten. Interestingly, these speleothems also show extreme variability in δ^{234}U, which directly reflects the α-recoil-controlled ^{234}U/^{238}U compositions found in their groundwater source, as discussed in Section 1. The ^{234}U/^{238}U and ^{235}U/^{238}U values are plotted against each other in Fig. 5. Despite the fact that ε^{235}U and δ^{234}U need not be correlated due to the dominant mass-independent effect of α-recoil combined with ongoing ^{234}U-decay on the ^{234}U/^{238}U signature, a positive correlation is found between ^{234}U/^{238}U and ^{235}U/^{238}U, dominated by samples showing the most extreme isotopic compositions. The only two samples displaying negative δ^{234}U are also characterized by the most negative ε^{235}U. For example, the KOZ speleothem has a negative ε^{235}U centred about −3.7ε and a negative δ^{234}U of −465‰. Note that the widely utilized CRM 145 U metal standard has, by definition in this study, an ε^{235}U of zero and a δ^{234}U centred about −37‰. These "negative" data points contrast sharply with the observations for all other samples, which are characterized by positive ε^{235}U and δ^{234}U values. For example, the speleothem sampled from Argentarola, Italy, is characterized by an ε^{235}U of +4.2ε and a δ^{234}U of +468‰, and the chimney deposit also displays positive ε^{235}U and δ^{234}U values of +8.3ε and +239‰, respectively.

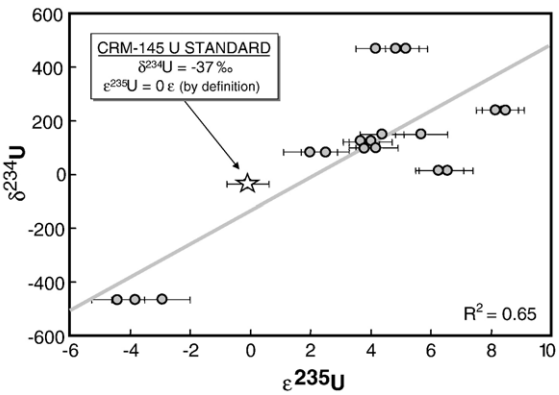

Fig. 5. ε^{235}U versus δ^{234}U for the suite of low-temperature terrestrial samples displayed in Fig. 4. Only samples of late-Quaternary age are shown, whereby the observed radioactive disequilibrium between ^{234}U and ^{238}U is likely to have been inherited during the same event that could potentially fractionate ^{235}U from ^{238}U. Older samples formed prior to ~500 ka will either display non-unique δ^{234}U signatures approaching radioactive equilibrium or δ^{234}U compositions that have shifted to new, unrelated values during subsequent fractionation events. Note the positive correlation between ^{234}U/^{238}U and ^{235}U/^{238}U.

The question then arises: By which mechanism(s) can ^{234}U/^{238}U disequilibria and ^{235}U/^{238}U fractionation plausibly be linked? Weathering by groundwater leaching could be a mechanism by which both (a) recoil-produced ^{234}U located outside the crystal lattice or in damaged lattice sites and (b) isotopically light lattice-bound ^{235}U could be preferentially leached from the mineral surface and released into the aquifer system over ^{238}U. Clearly, α-recoil is the dominant process controlling percent-level ^{234}U/^{238}U variability, but mass-dependent and nuclear field shift fractionations of ^{234}U/^{238}U and ^{235}U/^{238}U may act in addition, creating smaller epsilon- to permil-level isotopic shifts as a second-order effect caused by groundwater leaching.

5. Low-temperature abiotic experiments

5.1. Sequential leaching experiments

In an attempt to systematically investigate the likelihood of mineral weathering via groundwater leaching as a mechanism to fractionate ^{235}U from ^{238}U, a series of experiments were conducted in which single crystals were subjected to a series of sequential acid leaching steps (Fig. 6). Importantly, these experiments targeted U-rich minerals containing "metamict" zones that have been damaged by radioactive decay and are susceptible to weathering. Our expectation was that sequential acid leaching of these damaged zones would provide a means to preferentially release α-recoiled ^{234}U (and potentially ^{235}U) over ^{238}U from the crystal lattice, thus mimicking the mechanism by which ^{234}U is preferentially released into natural groundwaters, and giving rise to anomalously high ^{234}U/^{238}U in these systems. More "common" minerals hosting the majority of U in the Earth's crust but at relatively low concentrations, such as pyroxene and feldspar, were not targeted in the present study because they are expected to release "bulk" unfractionated U during sequential acid leaching. Single crystals of euxenite ([Y, Ca, Ce, U, Th][Nb, Ta, Ti]$_2$O$_6$), uraninite (UO$_2$), and zircon (ZiSiO$_4$) were selected for this purpose. The euxenite and zircon were extracted from 900 million year-old pegmatites sampled from the Evje–Iveland pegmatite field in southern Norway (Larsen et al., 2004). The uraninite was sampled from the uranium ore deposit at St. Joachimsthal, Czech Republic. The following sequential dissolution procedure was employed for the euxenite: (1) 0.1 N HNO$_3$; (2) 0.7 N HNO$_3$; (3) 1.4 HNO$_3$;

(4) 9 N HCl-1; (5) 9 N HCl-2; and (6) HNO_3–HCl–HF. The final HNO_3–HCl–HF acid digestion step did not result in complete dissolution of the euxenite, as a residue remained. The uraninite and zircon were subjected to the first three nitric acid leach steps only. The uraninite then underwent total dissolution with HNO_3-trace HF. The results for each mineral are displayed in Fig. 6.

In the case of the uraninite, no variation in ε^{235}U is observed between any of the sequential acid leachates with respect to the bulk sample, and all leachates display a mean ε^{235}U value centred about $+1\varepsilon$, with respect to CRM 145. Similarly for the zircon, all three HNO_3 leachates display ε^{235}U values that are identical, within error, to the mean value of the high-temperature samples, but are systematically offset from CRM 145 by $+5\varepsilon$.

In contrast, the results for the euxenite show no fractionation between ^{238}U and ^{235}U for any of the HNO_3 leaches, yielding a mean ε^{235}U of $+6\varepsilon$, but a systematic shift towards more elevated ε^{235}U is observed for the subsequent leach steps. In particular, the second HCl (b) leachate and the bulk sample have identical ε^{235}U centred about $+11\varepsilon$, $\sim 4\varepsilon$ higher than corresponding values for the initial nitric acid leachates. Given that total dissolution of the euxenite did not occur, this systematic progression towards higher ε^{235}U values may reflect either the preferential release of the lighter and, by inference, more loosely bound ^{235}U from the crystal lattice over heavier ^{238}U or, alternatively, the progressive dissolution of different mineral zones, each characterized by a distinct ε^{235}U composition. These experiments demonstrate that the selective leaching of minerals during low-temperature weathering is a possible mechanism by which ^{235}U and ^{238}U can be fractionated in near-surface terrestrial environments.

5.2. Oxidation–reduction experiments

Mineral leaching aside, it has been proposed that isotopic fractionation of ^{235}U/^{238}U could also occur at equilibrium via the redox chemistry of U (Bigeleisen, 1996; Schauble, 2007). For example, isotopic fractionations of U during the U(IV)–U(VI) exchange reaction have been artificially induced during laboratory anion exchange chromatography. These isotopic shifts have been attributed to nuclear field shift effects (Nomura et al., 1996), whereby heavy isotope enrichment is predicted to occur in the reduced U(IV)-bearing species with respect to the oxidized U(VI)-bearing species (Schauble, 2007). In

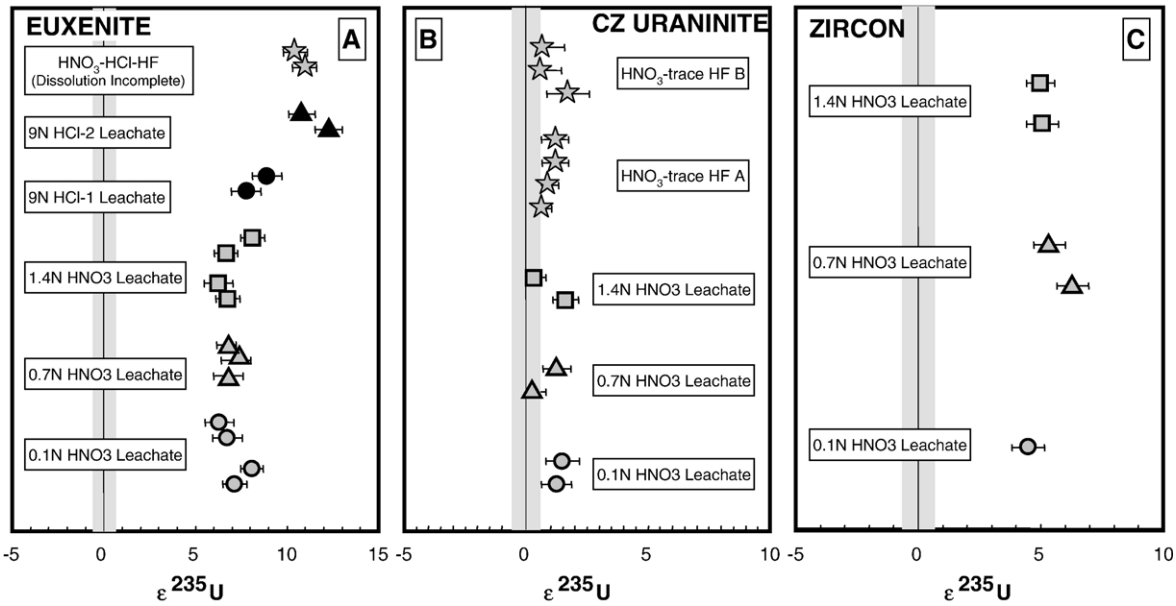

Fig. 6. ε^{235}U for a series of leaching experiments performed on (A) euxenite, (B) uraninite and (C) zircon. Reagents of progressing strength were used to sequentially dissolve distinct zonations within the mineral with potentially varying ε^{235}U or to selectively release ^{235}U (or ^{238}U) from the crystal lattice. The following sequential dissolution procedure was employed for the euxenite: (1) 0.1 N HNO_3; (2) 0.7 N HNO_3; (3) 1.4 N HNO_3; (4) 9 N HCl-1; (5) 9 N HCl-2; and (6) HNO_3–HCl–HF. The final HNO_3–HCl–HF acid digestion step did not result in complete dissolution of the euxenite, as a residue remained. The uraninite and zircon were subjected to the first three nitric acid leach steps only. The uraninite then underwent total dissolution with HNO_3-trace HF. A and B denote independently dissolved fragments of the same sample. The 2σ external reproducibility of the CRM 145 standard for a comparable U load size (represented by the shaded band) is shown for reference.

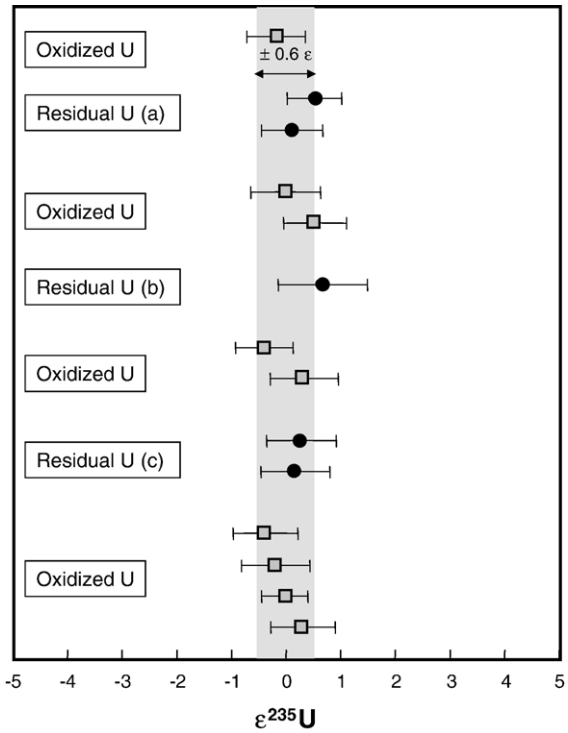

Fig. 7. ε^{235}U for repeat U redox experiments, in which zero-valent zinc was used to reduce U(VI) to U(IV) in an aliquot of the CRM 145 U standard with a U concentration of 80 ppb. Following reduction, the concentration of U in the residual solution was found to be 32 ppb, implying that approximately 60% of the soluble U(VI) was reduced to insoluble U(IV) and removed from the solution. No fractionation of ε^{235}U was observed at the 0.6ε level. The 2σ external reproducibility of the CRM 145 U standard for a comparable U load size (represented by the shaded band) is shown for reference.

several of the samples analyzed in the present study, oxidation–reduction processes could have instigated shifts in ^{235}U/^{238}U. In particular, groundwaters passing a U(VI)–U(IV) redox front can precipitate U during speleogenesis, offering the potential to fractionate ^{235}U from ^{238}U.

In order to assess the readiness with which ^{235}U can be fractionated from ^{238}U during the U(VI)–U(IV) redox transition in the natural environment, zero-valent zinc, a strong reductant, was used to reduce U(VI) to U(IV) in an 80 ppb U aliquot of the CRM 145 U standard, dissolved in milli-Q H_2O to yield a pH of 5.5. Zinc metal was then admixed to this standard and the redox reaction between the two species, U and Zn, as indicated below in (3), was allowed to proceed for 3 h, after which time the U solution was removed for subsequent chemical separation and isotopic analysis. The concentration of U in the residual solution was found to be 32 ppb, implying that approximately 60% of the soluble U(VI) was reduced to insoluble U(IV) and removed from the solution.

$$Zn^0 + U^{6+} \rightarrow U^{4+} + Zn^{2+} \quad (3)$$

The experiment was repeated twice. In each case, no fractionation of ε^{235}U was observed at the 0.4-ε level (Fig. 7).

The above-mentioned experiment may imply that other processes are more important than oxidation–reduction in fractionating U isotopes in the natural terrestrial environment. This result is supported by an independent experiment utilizing zero-valent iron to reduce U(VI) to U(IV) in a solution of equal atom U-500 standard (^{235}U/^{238}U ~ 1), which also failed to show any resolvable isotopic fractionation of ^{235}U from ^{238}U (Rademacher et al., 2006). Alternatively, the fast (<3 h) reaction rates characterizing the reduction of U(VI) to U (IV) may instead imply that both experiments were controlled by a rapid kinetic process associated with the preferential reduction of the lighter ^{235}U isotope with respect to heavy ^{238}U, as opposed to a slow equilibrium reaction during the exchange of aqueous U(VI) with solid U(IV). Additional experiments should therefore be

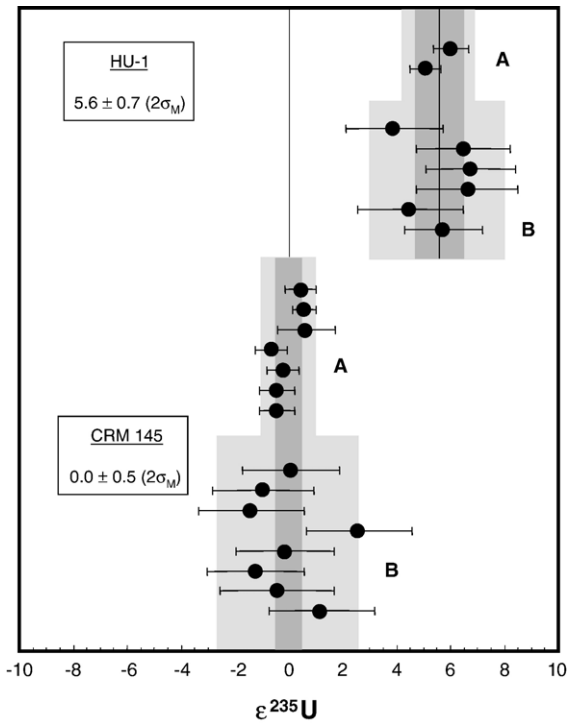

Fig. 8. ε^{235}U for the U isotopic standards CRM 145 U metal and the Harwell HU-1 uraninite that are commonly utilized in U-series isotopic protocols. The light and dark grey bands represent the 2σ external reproducibility and the error in the mean (2σ_M), respectively.

conducted at equilibrium to further investigate the potential of ε^{235}U fractionation during the redox transition from U(VI) to U (IV).

6. Natural variability in ^{235}U/^{238}U and the accuracy of the uranium decay series chronometers

Our results for low-temperature samples display significant epsilon-level deviations in ^{235}U/^{238}U away from the expected value constrained by measurements of 'high-temperature' samples (Stirling et al., 2005; Stirling et al., 2006). The most extreme ε^{235}U compositions to date are evidently recorded in Quaternary-aged speleothems, which show a $\sim 13\varepsilon$ variation in ε^{235}U, exceeding the analytical reproducibility by more than an order of magnitude. Compositions that are both heavier and lighter than the "normal" value, by 4ε and 9ε respectively, are observed. Speleothems are commonly utilized in paleoclimate research and natural variability in their ^{235}U/^{238}U composition will thus have a direct impact on their assigned U-series (Richards et al., 1994; Bard et al., 2002; Spoetl et al., 2002), ^{235}U–^{231}Pa (Edwards et al., 1997) and U–Th–Pb (Richards et al., 1998) chronologies. The impact of these new observations on the uranium decay series chronometers, all of which currently assume an invariant ^{235}U/^{238}U composition, is discussed in turn below.

6.1. The U-series chronometers

The ^{238}U–^{234}U–^{230}Th or U-series chronometer is based on the radiogenic in-growth of ^{230}Th with a characteristic half-life of 76,000 years towards secular equilibrium with its ^{238}U parent nuclide. The re-establishment of equilibrium between any excesses (or depletions) of ^{234}U ($t_{1/2}$=245,000 years) with respect to ^{238}U is also considered. The U-series age of a sample can thus be determined if the ^{234}U/^{238}U and ^{230}Th/^{238}U atomic ratios can be accurately measured. During ^{234}U/^{238}U and ^{230}Th/^{238}U measurement by mass spectrometry, it is normal to correct all ratios for permil- to percent-level instrumental mass fractionation effects using the measured ^{238}U/^{235}U normalized to the nominal "true" value of 137.88. There is scope to shift the ^{234}U/^{238}U and ^{230}Th/^{238}U determinations away from the correct values if the assumed 137.88 value for ^{238}U/^{235}U is incorrect and the systematics by which this occurs is discussed in detail in the Supplementary materials section. Taking the Quaternary speleothem observations as an example, a +1‰ shift in ^{235}U/^{238}U results in ^{234}U/^{238}U and ^{230}Th/^{238}U determinations that depart from their true values by 1.5‰, and offsets in the ^{230}Th-age of up to 40 years at 30 ka, 200 years at 100 ka, 2000 years at 300 ka, and 14,000 years at 500 ka. The excursion in the ^{230}Th-age can be amplified further through additional sources of isotopically "anomalous" ^{235}U/^{238}U inherent to the choice of U-series standard(s) adopted for calibration purposes (Fig. 8). For example, the commonly utilized U-series standard CRM 145 (assigned by definition an ε^{235}U of zero) has an anomalous ε^{235}U composition of -4.6ε with respect to the average terrestrial composition, leading to potential offsets in the U-series age of up to 20 years at 30 ka, 100 years at 100 ka, 1200 years at 300 ka, and 8000 years at 500 ka when it is used to calibrate the Faraday-electron multiplier relative gain. Importantly, if calibrations based on an isotopically anomalous standard are applied to an isotopically anomalous sample, and the ε^{235}U values characterizing both sample and standard are offset in the same direction towards anomalous values, then the net result will be to amplify the shift in the ^{230}Th-age. In contrast, if the offset in ε^{235}U experienced by the sample is of opposite sign to that exhibited by the standard, then the result will be to reduce the shift in the ^{230}Th-age.

In addition, both ^{234}U/^{238}U and ^{230}Th/^{238}U are critical input parameters in the determination of the sample's initial ^{234}U/^{238}U composition, a parameter that is widely utilized for determining U-series age reliability, particularly in fossil corals, for which the initial ^{234}U/^{238}U is well constrained. The results of this study show that corals have "normal" ε^{235}U values. However, the ^{235}U/^{238}U composition of other marine samples employing an initial ^{234}U/^{238}U criterion remains to be characterized and potential offsets of 2‰ at 100 ka can be incurred, assuming a 1‰ excursion in ε^{235}U. The initial ^{234}U/^{238}U can be offset from the correct value by 1‰ at 100 ka if the isotopically anomalous CRM 145 uranium standard is used for calibration purposes without cross-reference to a standard with a normal ε^{235}U composition, and this latter point is also relevant for fossil coral data (see the Supplementary material for a detailed discussion).

These anomalous shifts in the U-series age (and initial ^{234}U/^{238}U) determinations are comparable in magnitude to typical conventional U-series age uncertainties, and may bias the inferences drawn from a specific dataset, particularly when those constraints are based upon the statistical mean of a cluster of data points. Natural variability in ^{235}U/^{238}U will have a significant impact on the increasing range of protocols that are being developed to measure the U-series isotopes with progressively higher levels of precision (Andersen et al., 2004; Potter et al., 2005a; Stirling et al., 2005; Stirling et al., 2006).

Similar excursions in age can occur for the ^{231}Pa chronometer in the presence of isotopically anomalous

ε^{235}U, which is also derived assuming ^{238}U/^{235}U is invariant and equal to 137.88.

6.2. The U–Th–Pb chronometer

The U–Th–Pb chronometers are based on the in-growth of stable ^{206}Pb and ^{207}Pb from their respective long-lived parent nuclides, ^{238}U ($t_{1/2}$=4.5 billion years) and ^{235}U ($t_{1/2}$=700 million years). Natural variability in ε^{235}U will have a direct bearing on the accuracy of ^{207}Pb/^{206}Pb (or Pb–Pb) ages in particular, which assume concordance between the ^{238}U–^{206}Pb and ^{235}U–^{207}Pb decay series, linked by the critical assumption that ^{238}U/^{235}U is equal to 137.88 across the entire solar system. The ε^{235}U results presented here and in Stirling et al. (2005, 2006) for high-temperature meteorite samples show no variation at the 1ε level. The outlook also appears promising for terrestrial samples formed in high-temperature environments; none of the samples analyzed to date displays well-resolvable deviations in ε^{235}U away from "normal" compositions, although this should be verified with additional data to expand the existing dataset. The apparent absence of isotopic fractionation effects in meteoritic ^{235}U/^{238}U verifies that models of solar system formation constrained by Pb–Pb relative age differences of only a few million years (Amelin et al., 2002; Amelin, 2005; Baker et al., 2005) are likely to be robust and not require revision. Furthermore, the calibration of other radiometric chronometers, such as the lutetium–hafnium (^{176}Lu–^{176}Hf) system, against the Pb–Pb system (Scherer et al., 2001) appears justified for samples formed in high-temperature environments.

In contrast to the high-temperature systems, Pb–Pb ages derived for low-temperature samples may, in some instances, need to be reconsidered. In the present study, this is highlighted by the results for Quaternary speleothems. Specifically, a 1‰ deviation in ε^{235}U away from the expected value of 137.88 translates to a deviation in the Pb–Pb age away from the true age of ~2.3 million years in 100 million year-old samples, ignoring potential additional sources of error introduced by calibration procedures. In 4.5 billion year-old samples, a ^{235}U/^{238}U shift of this magnitude would offset the Pb–Pb age from the true age by ~1.4 million years.

6.3. The Cm–U cosmochronometer

The Cm–U cosmochronometer is based on the α-decay of presently extinct ^{247}Cm to ^{235}U with a half-life of 15.6 Myr. The presence of "live" ^{247}Cm in the early solar system should be manifested today as small variations in ^{235}U/^{238}U in primitive meteorite material. The ^{247}Cm–^{235}U system thus offers the potential to elucidate the formation and evolution of the early solar system, provided that no addition (or removal) of ^{235}U occurs other than via ^{247}Cm decay. In terms of validating this assumption, the outlook for this recently revisited chronometer appears promising, as no resolvable fractionations of ^{235}U/^{238}U have been observed in meteoritic material to date (Stirling et al., 2005; Stirling et al., 2006).

7. Concluding remarks

Using a Nu Instruments Nu Plasma MC-ICPMS, we have measured ε^{235}U in a suite of low-temperature samples formed in a wide range of marine and continental near-surface terrestrial environments. A high-purity ^{233}U–^{236}U mixed spike was utilized to internally monitor instrumental mass fractionation. ε^{235}U was determined at the 0.4ε level (2σM) on samples comprising 50 ng of ^{238}U. The natural variability in ε^{235}U shown by the analyzed samples is ~13ε, and exceeds the analytical reproducibility by more than an order of magnitude. Compositions that are both heavier and lighter than the "normal" value by 4ε and 9ε respectively, are observed. In the present dataset, the greatest variability in ε^{235}U is displayed by speleothems precipitated from groundwaters. Possible mechanisms to account for this fractionation were explored in the context of abiotic fractionation processes. Specifically, sequential leaching experiments of U-rich minerals indicate that mineral weathering is a possible mechanism by which ^{235}U can be fractionated from ^{238}U in groundwaters. In contrast, the role of redox processes in fractionating ^{235}U from ^{238}U remains uncertain, as experiments utilizing zero-valent zinc to promote the redox transition of U(VI) to U(IV) yielded a ~60% reduction of U without shifting ^{235}U/^{238}U towards anomalous values. The results of these redox experiments may require confirmation, as they may be influenced by a fast kinetic reaction rather than a slow equilibrium process.

Isotopic fractionation of ^{238}U from ^{235}U has broad implications for low-temperature geochemistry. In contrast to the lighter stable isotope systems, which can be readily fractionated in a wide range of environmental and geological environments, uranium's heavy atomic mass may limit the range of processes by which it can be fractionated. Thus, U may potentially offer new insight into the processes at work during low-temperature biotic, abiotic and redox processing, as has been investigated in recent years for the heavy stable isotope systematics of the element thallium (Rehkämper et al., 2002; Rehkämper et al., 2004; Nielsen et al., 2005; Nielsen et al., 2006). For example, U is linked with elements such as Fe during redox processing (Gu et al.,

1998; Duff et al., 2002), and coupled measurements of $^{235}U/^{238}U$ and Fe isotopic composition may provide useful information on oxidation–reduction mechanisms.

With regard to geochronology, the U-series and ^{235}U–^{231}Pa chronometers, and more recently the U–Th–Pb chronometer, have been widely applied to low-temperature samples for paleoclimate research. One can envisage that for a 300,000 year-old speleothem, characterized by a $^{235}U/^{238}U$ that departs from the expected value by 10ε, that anomalous shifts in the U-series age in excess of 2,000 years towards younger or older values could occur if $^{235}U/^{238}U$ has not been correctly characterized during every calculation step. Similar fractional deviations in the calculated age away from the true sample age would be expected for other time periods. Age biases of this magnitude could bias our understanding of the mechanisms driving Quaternary climate change, particularly as U-series analysis protocols move towards progressively higher levels of precision. Chronology aside, low-temperature variability in $^{235}U/^{238}U$ will have a direct bearing on the utilization of the U decay series nuclides as tracers of past and present environmental conditions.

These limitations can, in large part, be overcome by the utilizing a ^{236}U–^{233}U double spike with a well-characterized $^{236}U/^{233}U$ for the purpose of monitoring the instrumental mass fractionation factor, in place of the "natural" $^{238}U/^{235}U$ ratio, and by careful consideration of the standards adopted for calibration procedures.

Acknowledgements

We are grateful to the valuable support of Felix Oberli, Helen Williams and Sarah Woodland, as well as Urs Menet, Heiri Baur and Bruno Rütsche, who expended time and effort to ensure the smooth running of the MC-ICPMS facilities in IGMR. We especially thank Bill Thompson and Sune Nielsen for their careful and insightful reviews which helped improve the manuscript. We thank Don Porcelli, Per Andersson, Sune Nielsen, Mark Rehkämper, Vitor Magalhaes, Christoph Spötl, and Fabrizio Antonioli who kindly provided access to samples. We are also grateful to Don Porcelli, Per Andersson and the Swedish Polar Research Secretariat for providing access to the seawater samples.

Appendix A. Supplementary data

Supplementary data associated with this article can be found, in the online version, at doi:10.1016/j.epsl.2007.09.019.

References

Amelin, Y., 2005. Meteorite phosphates show constant ^{176}Lu decay rate since 4557 million years ago. Science 310, 839–841.

Amelin, Y., Krot, A.N., Hutcheon, I.D., Ulyanov, A.A., 2002. Lead isotopic ages of chondrules and calcium–aluminum-rich inclusions. Science 297, 1678–1683.

Anbar, A.D., 2004. Iron stable isotopes: beyond biosignatures. Earth Planet. Sci. Lett. 217, 223–236.

Andersen, M.B., Stirling, C.H., Porcelli, D., Halliday, A.N., Andersson, P.S., Baskaran, M., 2007. The tracing of riverine U in Arctic seawater with very precise $^{234}U/^{238}U$ measurements. Earth Planet. Sci. Lett. 259, 171–185.

Andersen, M.B., Stirling, C.H., Potter, E.-K., Halliday, A.N., 2004. Toward epsilon levels of measurement precision on $^{234}U/^{238}U$ by using MC-ICPMS. Int. J. Mass Spectrom. 237, 107–118.

Andersson, P., Wasserburg, G.J., Chen, J.H., Papanastassiou, D.A., Ingri, J., 1995. ^{238}U–^{234}U and ^{232}Th–^{230}Th in the Baltic Sea and in river water. Earth Planet. Sci. Lett. 130, 217–234.

Andersson, P., Wasserburg, G.J., Ingri, J., 1992. The sources and transport of Sr and Nd isotopes in the Baltic Sea. Earth Planet. Sci. Lett. 113, 459–472.

Andersson, P.S., Porcelli, D., Wasserburg, G.J., Ingri, J., 1998. Particle transport of ^{234}U–^{238}U in the Kalix River and in the Baltic Sea. Geochim. Cosmochim. Acta 62, 385–392.

Baker, J., Bizzarro, M., Wittig, N., Connelly, J., Haack, H., 2005. Early planetesimal melting from an age of 4.5662 Gyr for differentiated meteorites. Nature 436, 1127–1131.

Bard, E., Antonioli, F., Silenzi, S., 2002. Sea-level during the penultimate interglacial period based on a submerged stalagmite from Argentarola Cave (Italy). Earth Planet. Sci. Lett. 196, 135–146.

Bard, E., Fairbanks, R.G., Hamelin, B., Zindler, A., Hoang, C.T., 1991. Uranium-234 anomalies in corals older than 150,000 years. Geochim. Cosmochim. Acta 55, 2385–2390.

Belshaw, N.S., Freedman, P.A., O'Nions, R.K., Frank, M., Guo, Y., 1998. A new variable dispersion double-focusing plasma mass spectrometer with performance illustrated for Pb isotopes. Int. J. Mass Spectrom. 181, 51–58.

Bigeleisen, J., 1996. Nuclear size and shape effects in chemical reactions. Isotope chemistry of the heavy elements. J. Am. Chem. Soc. 118, 3676–3680.

Bigeleisen, J., Mayer, M.J., 1947. Calculation of equilibrium constants for isotopic exchange reactions. J. Chem. Phys. 15, 261–267.

Chen, J.H., Edwards, R.L., Wasserburg, G.J., 1986. ^{238}U, ^{234}U and ^{232}U in sea water. Earth Planet. Sci. Lett. 80, 241–251.

Chen, J.H., Wasserburg, G.J., 1980. A search for isotopic anomalies in uranium. Geophys. Res. Lett. 7 (4), 275–278.

Chen, J.H., Wasserburg, G.J., 1981. The isotopic composition of uranium and lead in Allende inclusions and meteoritic phosphates. Earth Planet. Sci. Lett. 52, 1–15.

Cheng, H., Edwards, L.R., Hoff, J., Gallup, C.D., Richards, D.A., Asmerom, Y., 2000. The half-lives of uranium-234 and thorium-230. Chem. Geol. 169, 17–33.

Cowan, G.A., Adler, H.H., 1976. The variability of the natural abundance of ^{235}U. Geochim. Cosmochim. Acta 40, 1487–1490.

DeCelles, P.G., Gehrels, G.E., Quade, J., LaReau, B., Spurlin, M., 2000. Tectonic implications of U–Pb zircon ages of the Himalayan Orogenic Belt in Nepal. Science 288, 497–499.

Delanghe, D., Bard, E., Hamelin, B., 2002. New TIMS constraints on the uranium-238 and uranium-234 in seawaters from the main ocean basins and the Mediterranean Sea. Mar. Chem. 80, 79–93.

DePaolo, D.J., Maher, K., Christensen, J.C., McManus, J.F., 2006. Sediment transport time measured with U-series isotopes: results from ODP North Atlantic drift site 984. Earth Planet. Sci. Lett. 248, 394–410.

Duff, M.C., Urbanik Coughlin, J., Hunter, D.B., 2002. Uranium co-precipitation with iron oxide minerals. Geochim. Cosmochim. Acta 66, 3533–3547.

Edwards, L.R., Chen, J.H., Wasserburg, G.J., 1987. ^{238}U–^{234}U–^{230}Th–^{232}Th systematics and the precise measurement of time over the past 500 000 years. Earth Planet. Sci. Lett. 81, 175–192.

Edwards, L.R., Cheng, H., Murrell, M.T., Goldstein, S.J., 1997. Protactinium-231 dating of carbonates by thermal ionization mass spectrometry: implications for Quaternary climate change. Science 276, 782–786.

Esat, T.M., McCulloch, M.T., Chappell, J., Pillans, B., Omura, A., 1999. Rapid fluctuations in sea level recorded at Huon Peninsula during the Penultimate Deglaciation. Science 283, 197–201.

Gallup, C.D., Cheng, H., Taylor, F.W., Edwards, R.L., 2002. Direct determination of the timing of sea level change during Termination II. Science 295, 310–313.

Gallup, C.D., Edwards, R.L., Johnson, R.G., 1994. The timing of high sea levels over the past 200,000 years. Science 263, 796–800.

Goldstein, S.J., Stirling, C.H., 2003. Techniques for measuring uranium-series nuclides: 1992–2002. Uranium-Series Geochemistry vol. 52, 23–57.

Gu, B., Liang, L., Dickey, M.J., Yin, X., Dai, S., 1998. Reductive precipitation of uranium(VI) by zero-valent iron. Environ. Sci. Technol. 32, 3366–3373.

Habfast, K., 1998. Fractionation correction and multiple collectors in thermal ionization isotope ratio mass spectrometry. Int. J. Mass Spectrom. 176 (1–2), 133–148.

Halliday A.N., Stirling C.H., Freedman P.A., Oberli F., Reynolds B., and Georg R.B. in press. High precision isotope ratio measurements using multiple collector inductively coupled plasma mass spectrometry. In Encyclopedia of Mass Spectrometry, vol. 5.

Hart, S.R., Zindler, A., 1989. Isotope fractionation laws—a test using calcium. Int. J. Mass Spectrom. 89 (2–3), 287–301.

Ivanovich, M., Harmon, R.S., 1992. Uranium-series Disequilibrium: Applications to earth, marine and environmental sciences. Clarendon Press, Oxford.

Kigoshi, K., 1971. Alpha recoil thorium-234: dissolution into water and uranium-234/uranium-238 disequilibrium in nature. Science 173, 47–48.

Larsen, R.B., Henderson, I., Ihlen, P.M., Jacamon, F., 2004. Distribution and petrogenic behaviour of trace elements in granitic pegmatite quartz from South Norway. Contrib. Mineral. Petrol. 147, 615–628.

Lundstrom, C.C., 2003. Uranium-series disequilibria in mid-ocean ridge basalts: observations and models of basalt genesis. In: Bourdon, B., Henderson, G.M., Lundstrom, C.C., Turner, S. (Eds.), Uranium-Series Geochemistry, vol. 52. Mineralogical Society of America, pp. 175–214.

Luo, X., Rehkämper, M., Lee, D.-C., Halliday, A.N., 1997. High precision ^{230}Th/^{232}Th and ^{234}U/^{238}U measurements using energy-filtered ICP magnetic sector multiple collector mass spectrometry. Int. J. Mass Spectrom. Ion Process. 171, 105–117.

Marechal, C., Albarede, F., 2002. Ion-exchange fractionation of copper and zinc isotopes. Geochim. Cosmochim. Acta 66 (9), 1499–1509.

Nielsen, S.G., Rehkämper, M., Norman, M.D., Halliday, A.N., Harrison, D., 2006. Thallium isotopic evidence for ferromanganese sediments in the mantle source of Hawaiian basalts. Nature 439 (7074), 314–317.

Nielsen, S.G., Rehkämper, M., Porcelli, D., Andersson, P., Halliday, A.N., Swarzenski, P.W., Latkoczy, C., Günther, D., 2005. Thallium isotope composition of the upper continental crust and rivers—an investigation of the continental sources of dissolved marine thallium. Geochim. Cosmochim. Acta 69 (8), 2007–2019.

Nomura, M., Higuchi, N., Fujii, Y., 1996. Mass dependence of uranium isotope effects in the U(IV)–U(VI) exchange reaction. J. Am. Chem. Soc. 118, 9127–9130.

Nutman, A.P., Mojzsis, S.J., Friend, C.R.L., 1997. Recognition of >3850 Ma water-lain sediments in West Greenland and their significance for the early Archaean Earth. Geochim. Cosmochim. Acta 61, 2475–2484.

Potter, E.-K., Stirling, C.H., Andersen, M.B., Halliday, A.N., 2005a. High precision Faraday collector MC-ICPMS thorium isotope ratio determination. Int. J. Mass Spectrom. 247, 10–17.

Potter, E.K., Stirling, C.H., Andersen, M.B., Halliday, A.N., 2005b. High precision Faraday collector MC-ICPMS thorium isotope ratio determination. Int. J. Mass Spectrom. 247 (1–3), 10–17.

Proceedings of an International Symposium on the Oklo Phenomenon, 1975. IAEA, French Atomic Energy Commission and Government of the Republic of Gabon, Libreville, 23–27 June.

Rademacher, L.K., Lundstrom, C.C., Johnson, T.M., Sanford, R.A., Zhao, J., Zhang, Z., 2006. Experimentally determined uranium isotope fractionation during reduction of hexavalent U by bacteria and zero valent iron. Environ. Sci. Technol. 40, 6943–6948.

Rehkämper, M., Frank, M., Hein, J.R., Halliday, A., 2004. Cenozoic marine geochemistry of thallium deduced from isotopic studies of ferromanganese crusts and pelagic sediments. Earth Planet. Sci. Lett. 219 (1–2), 77–91.

Rehkämper, M., Frank, M., Hein, J.R., Porcelli, D., Halliday, A., Ingri, J., Liebetrau, V., 2002. Thallium isotope variations in seawater and hydrogenetic, diagenetic, and hydrothermal ferromanganese deposits. Earth Planet. Sci. Lett. 197, 65–81.

Rehkämper, M., Nielsen, S.G., 2004. The mass balance of dissolved thallium in the oceans. Mar. Chem. 85 (3–4), 125–139.

Rehkämper, M., Schonbachler, M., Stirling, C.H., 2001. Multiple collector ICP-MS: Introduction to instrumentation, measurement techniques and analytical capabilities. Geostandards Newsletter 25 (1), 23–40.

Reynolds, B.C., Wasserburg, G.J., Baskaran, M., 2003. The transport of U- and Th-series nuclides in sandy confined aquifers. Geochim. Cosmochim. Acta 67 (11), 1955–1972.

Richards, D.A., Bottrell, S.H., Cliff, R.A., Stroehle, K., Rowe, P.J., 1998. U–Pb dating of a speleothem of Quaternary age. Geochim. Cosmochim. Acta 62, 3683–3688.

Richards, D.A., Smart, P.L., Edwards, R.L., 1994. Maximum sea levels for the last glacial period from U-series ages of submerged speleothems. Nature 367, 357–360.

Richet, P., Bottinga, Y., Javoy, M., 1977. A review of hydrogen, carbon, nitrogen, oxygen, sulphur, and chlorine stable isotope fractionation among gaseous molecules. Annu. Rev. Earth Planet. Sci. 5, 65–110.

Robinson, L.F., Belshaw, N.S., Henderson, G.M., 2004a. U and Th concentrations and isotope ratios in modern carbonates and waters from the Bahamas. Geochim. Cosmochim. Acta 68, 1777–1789.

Robinson, L.F., Henderson, G.M., Hall, L., Matthews, I., 2004b. Climatic control of riverine and seawater uranium-isotope ratios. Science 305, 851–854.

Robinson, L.F., Henderson, G.M., Slowey, N.C., 2002. U–Th dating of marine isotope stage 7 in Bahamas slope sediments. Earth Planet. Sci. Lett. 196, 175–187.

Schauble, E.A., 2007. Role of nuclear volume in driving equilibrium stable isotope fractionation of mercury, thallium, and the other very heavy elements. Geochim. Cosmochim. Acta 71, 2170–2189.

Scherer, E., Muenker, C., Mezger, K., 2001. Calibration of the lutetium–hafnium clock. Science 293, 683–687.

Smith, C.N., Kesler, S.E., Klaue, B., Blum, J.D., 2005. Mercury isotope fractionation in fossil hydrothermal systems. Geology 33, 825–828.

Spoetl, C., Mangini, A., Frank, N., Eichstaedter, R., Burns, S.J., 2002. Start of the last interglacial period at 135 ka: evidence from a high Alpine speleothem. Geology 30 (9), 815–818.

Steiger, R.H., Jaeger, E., 1977. Subcommission on geochronology: convention on the use of decay constants in geo- and cosmochronology. Earth Planet. Sci. Lett. 36, 359–362.

Stirling, C.H., Esat, T.M., Lambeck, K., McCulloch, M.T., 1998. Timing and duration of the Last Interglacial: evidence for a restricted interval of widespread coral reef growth. Earth Planet. Sci. Lett. 160, 745–762.

Stirling, C.H., Esat, T.M., Lambeck, K., McCulloch, M.T., Blake, S.G., Lee, D.-C., Halliday, A.N., 2001. Orbital forcing of the Marine Isotope Stage 9 interglacial. Science 291, 290–293.

Stirling, C.H., Esat, T.M., McCulloch, M.T., Lambeck, K., 1995. High-precision U-series dating of corals from Western Australia and implications for the timing and duration of the Last Interglacial. Earth Planet. Sci. Lett. 135, 115–130.

Stirling, C.H., Halliday, A.N., Porcelli, D., 2005. In search of live ^{247}Cm in the early solar system. Geochim. Cosmochim. Acta 69 (4), 1059–1071.

Stirling, C.H., Halliday, A.N., Potter, E.-K., Andersen, M.B., Zanda, B., 2006. A low abundance of ^{247}Cm in the early solar system and implications for r-process nucleosynthesis. Earth Planet. Sci. Lett. 251, 386–397.

Thompson, W.G., Goldstein, S.L., 2005. Open-system coral ages reveal persistent suborbital sea-level cycles. Science 308, 401–404.

Thompson, W.G., Goldstein, S.L., 2006. A radiometric calibration of the SPECMAP timescale. Quat. Sci. Rev. 25, 3207–3215.

Thompson, W.G., Spiegelman, M.W., Goldstein, S.L., Speed, R.C., 2003. An open-system model for U-series age determinations of fossil corals. Earth Planet. Sci. Lett. 210, 365–381.

Turner, S., Bourdon, B., Gill, J., 2003. Insights into magma genesis at convergent margins from U-series isotopes. In: Bourdon, B., Henderson, G.M., Lundstrom, C.C., Turner, S.P. (Eds.), Uranium-Series Geochemistry, vol. 52. Mineralogical Society of America, pp. 255–361.

Urey, H.C., 1947. The thermodynamic properties of isotopic substances. J. Chem. Soc. (London) 562–581.

Villemant, B., Feuillet, N., 2003. Dating open systems by the ^{238}U–^{234}U–^{230}Th method: application to Quaternary reef terraces. Earth Planet. Sci. Lett. 210, 105–118.

Winograd, I.J., Coplen, T.B., Landwehr, J.M., Riggs, A.C., Ludwig, K.R., Szabo, B.J., Kolesar, P.T., Revesz, K.M., 1992. Continuous 500,000-year climate record from vein calcite in Devils Hole, Nevada. Science 258, 255–260.

Xie, Q., Liu, S., Evans, D., Dillon, P., Hintelmann, H., 2005. High precision Hg isotope analysis of environmental samples using gold trap-MC-ICP-MS. J. Anal. At. Spectrom. 20, 515–522.